of spin density on the metal and eventually on the axial ligand.[6h] This may allow us to suggest that the electronic state of HRP compound I is more $^2A_{1u}$ like rather than $^2A_{2u}$, which has long been accepted on the basis of electronic absorption spectra and ENDOR results. ENDOR results of HRP compound I,[12] however, could be reasonably explained by assuming this compound to be in the $^2A_{1u}$ state, since the experimentally estimated average spin densities distributed on porphyrin nitrogen and carbon are very close to MO theoretical values calculated for an $^2A_{1u}$ radical.[7] Moreover, the meso proton coupling by the ENDOR experiment appears closer to the MO results for the $^2A_{1u}$ state if we assume that A^H has a negative sign. By analogy with the present studies on the porphyrin π-cation radical, the electronic state of the porphyrin π-cation of HRP compound I is likely formulated as $^2A_{1u}$ mixed to some extent with $^2A_{2u}$. This review has also been suggested by Stillman et al.[35] on the basis of their MCD results that there is no distinct difference in the MCD spectra of CAT and HRP compounds I, both of which do not resemble either of the MCD spectrum for typical $^2A_{1u}$ or $^2A_{2u}$ porphyrin π-cation radical. At any event, deuterium NMR examination of HRP compound I reconstituted with the meso deuterated protohemin could directly test our present speculation on the electronic state of this radical center, which is planned in our laboratory.

Keeping in mind the above discussion, we would like to make some comment on the NMR spectral features of HRP compound I. It was proposed that weak coupling between electron spins on iron(IV) and on the porphyrin radical results in enhanced electron spin relaxation, eventually leading to the sharp NMR and very broadened ESR spectra of HRP compound I.[8,36] However, the possibility of the enhanced electron spin relaxation caused by fast exchange between $^2A_{1u}$ and $^2A_{2u}$ porphyrin radical states should also be taken into account to explain the unique spectral features of NMR and ESR spectra of HRP compound I. This mixing mechanism could also be responsible for ambiguities in assigning their optical spectra to either $^2A_{1u}$ or $^2A_{2u}$ type. The subtle structural changes in the heme environments of HRP and CAT could modulate the mixing of two electronic states. Details of the studies of the π-cation radicals of ruthenium(II) meso and deuteroporphyrin monocarbonyl complexes and their derivatives incorporated into HRP will be published elsewhere.

Acknowledgment. The authors thank Drs. T. Kawamura and H. Ohya-Nishiguchi for helpful discussions. This work is supported by a grant from the Ministry of Education, Japan (57470119).

(35) Browett, W. R.; Stillman, M. J. *Biochim. Biophys. Acta* **1981**, *660*, 1-7. (b) Browrett, W. R.; Stillman, M. J. *Inorg. Chim. Acta* **1981**, *49*, 69-77.

(36) Morishima, I.; Ogawa, S. *J. Am. Chem. Soc.* **1978**, *100*, 7125-7128. (b) Morishima, I.; Ogawa, S. *Biochemistry* **1978**, 4384-4388. 4384-4388. (c) Morishima, I.; Ogawa, S. *Biochem. Biophys. Res. Commun.* **1978**, *83*, 946-953.

Low-Temperature ^{13}C Magnetic Resonance in Solids. 3. Linear and Pseudolinear Molecules

Alvin J. Beeler,[1] Anita M. Orendt, David M. Grant,* Peter W. Cutts, Josef Michl,* Kurt W. Zilm, John W. Downing, Julio C. Facelli, Michael S. Schindler,[2] and Werner Kutzelnigg[2]

Contribution from the Department of Chemistry, University of Utah, Salt Lake City, Utah 84112. *Received June 4, 1984*

Abstract: The solid-state low-temperature ^{13}C NMR spectra of five linear (CO, CO_2, OCS, C_3O_2, acetylene) and four pseudolinear (propyne, 2-butyne, allene, ketene) molecules have been obtained. The assignments of the shielding tensor axes are made from symmetry in all but allene and ketene. In these pseudolinear molecules shift assignments are based on ab initio calculations by the IGLO version of the coupled Hartree–Fock method. Except for carbon monoxide, the parallel component of the chemical shift tensor ($\sigma_\parallel$) for C_∞ is remarkably constant at -90 ppm from Me_4Si, establishing a reference point for discussing the paramagnetic shielding terms. Variations in both the diamagnetic term and off-center shielding terms of both varieties were found to be relatively small. Destruction of the C_∞ symmetry in molecules having hydrogen lying off the C–C axis of pseudolinear molecules resulted in major shifts in the tensorial shieldings. Theoretical correlation of the relative experimental shielding values is very good although the agreement of magnitudes in the low-field range worsens as one moves away from the methane shift which is used as a fiducial value to establish the comparison. It is concluded that the theory faithfully represents the shielding phenomena and may be used to assign shielding components to specific spatial orientations when symmetry features or other unequivocal information is lacking.

Recent NMR work[3-8] on small molecules at low temperatures has resulted from the pioneering work on cross polarization (CP) by Hartman and Hahn[9] and Pines, Gibby, and Waugh.[10] While the initial low-temperature work with ^{13}C CP experiments was conducted at liquid nitrogen temperatures, others[7,11] have extended the method to much lower temperatures using matrix isolation techniques developed earlier in optical and electron spin resonance spectroscopy.[12] Matrix isolation techniques in NMR have also benefited from the use of labeled compounds to enhance the signal-to-noise ratio and to provide information on the ^{13}C–^{13}C dipolar interaction. Isolation and immobilization of both reactive

(1) Present address: E. I. du Pont de Nemours & Co., Richmond, VA.
(2) Ruhr Universitat Bochum, Germany.
(3) Linder, J.; Hohener, A.; Ernst, R. R. *J. Magn. Reson.* **1979**, *35*, 379.
(4) Kohl, J. E.; Semack, M. G.; White D. *J. Chem. Phys.* **1978**, *69*, 5378.
(5) Pines, A.; Gibby, M. G.; Waugh, J. S. *J. Chem. Phys.* **1973**, *59*, 569.
(6) Gibson, A. A. V.; Scott, T. A.; Fukushima, E. *J. Magn. Reson.* **1977**, *27*, 29.
(7) Zilm, K. W.; Conlin, R. T.; Grant, D. M.; Michl, J. *J. Am. Chem. Soc.* **1980**, *100*, 6672.
(8) Ishol, L. M.; Scott, T. A. *J. Magn. Reson.* **1977**, *27*, 23.
(9) Hartman, S. R.; Hahn, E. L. *Phys. Rev.* **1962**, *128*, 2042.
(10) Pines, A.; Gibby, M. G.; Waugh, J. S. *Chem. Phys. Lett.* **1972**, *15*, 373.
(11) Zilm, K. W.; Grant, D. M. *J. Am. Chem. Soc.* **1981**, *103*, 2913.
(12) Moskovits, M., Ozin, G. A., Eds. "Cryochemistry"; John Wiley and Sons, Inc.: New York, 1976.

0002-7863/84/1506-7672$01.50/0

and stable molecular species in the inert argon environment constitute the principal advantages of the method.

Experimental information available for small linear or pseudolinear molecules is rather limited. Molecules which contain only hydrogen atoms off a C_∞ axis are refered to as pseudolinear. Pines[10,13] has measured the chemical shift anisotropy (CSA) for CS_2 and dimethylacetylene at liquid nitrogen temperature, while Scott and co-workers[6] have observed the CSA of ^{13}C-labeled CO at liquid helium temperatures.

The present study, repeating measurements on CO and dimethylacetylene, presents chemical shift tensors for five linear molecules, C_2H_2, CO, CO_2, OCS, and C_3O_2, and four pseudolinear molecules, $CH_3C{\equiv}CH$, $CH_3C{\equiv}CCH_3$, $CH_2{=}C{=}CH_2$, and $CH_2{=}C{=}O$. The literature values for CS_2 are included for comparison with CO_2 and OCS. Trends in principal values are discussed and related to theoretical calculations of chemical shielding.

Experimental and Computational Methods

Spectrometer. All spectra were obtained on a home-built spectrometer operating at 20.12 MHz for carbon-13 (^{13}C). The probe[14] used with this spectrometer contains a single coil which has been double tuned for both ^{13}C and ^1H frequencies and produces a rotating field of 50 kHz at the ^1H frequency with 100 W of power. The coil is barely large enough to accept a 12-mm NMR tube, thus permitting us to maximize the filling factor. This arrangement also permits the RF components to be maintained at room temperature, easing the refrigeration requirements on the cryogenic system. An external D_2O lock was used to maintain field stability.

Cryogenic Apparatus and Matrix Deposition. The cryogenic apparatus used for obtaining ^{13}C chemical shift spectra was assembled in this laboratory.[7] The cooling unit is an Air Products Model 202-B closed-cycle helium refrigerator. At 20 K this unit has a cooling capacity of 20 W. The cryotip is equipped with a Fe/Au thermocouple for temperature measurement and a resistive heater for operation above its lowest temperature limit.

Threaded into the cryotip is a 7.0-in.-long, 0.25-in.-diameter, indium-coated rod made of oxygen-free high-conductivity copper. Good thermal conductivity is maintained by use of an indium gasket and conductive grease between the copper rod and the cryotip. A 3.0-in.-long, 0.094-in.-diameter sapphire rod is pressed into the end of the copper rod. Indium solder was melted into the hole in the copper rod in order to ensure good thermal contact between the copper and the inserted sapphire. The difference in temperature measurement between the sample and the Fe/Au thermocouple which are separated by 10 in. is about 5 K.

This temperature gradient was estimated from the temperature at which solid argon sublimes from the sapphire rod or cryotip as the cryostat is allowed to warm up. Further comparisons with other cryostats that have been calibrated at a similar distance from the thermocouple indicate that the sample temperature is within 10 K of the measured temperature at the thermocouple.

The lower end of the cryotip is enclosed by a shroud constructed from nonmagnetic stainless steel. A glass envelope is inserted into a 0.75-in. Cajon vacuum fitting welded onto the end of the vacuum shroud. This envelope consists of 6 in. of 19-mm diameter Pyrex glass tubing which is joined to 2 in. of a 12-mm diameter NMR tube. The NMR tube was further connected to a vacuum line containing the sample by means of approximately 4 in. of 0.25-in.-diameter Pyrex glass tubing provided with a constriction, a U-shaped tube immersed in an ultrasonic water bath which ensures uniform mixing of the gas mixture to be deposited,[15] 12 in. of stainless steel flexible tubing, and a calibrated leak valve.

Prior to sample deposition, the vacuum shroud and glass envelope were evacuated to a pressure lower than 8×10^{-5} torr, at which point the closed-cycle refrigerator was turned on. The cryostat typically requires 2 h for the tip temperature to stabilize in the 15–20 K range. Final pressure is usually $2\text{–}4 \times 10^{-6}$ torr. Once the temperature has stabilized, the deposition is started by bleeding in the sample from the vacuum line, and a drop-shaped sample condenses on the end of the sapphire rod.

The deposition is terminated when the matrix reaches within 1.5 to 2 mm of the glass walls. The glass envelope is then sealed off at the constriction and the cryostat disconnected from the vacuum line and moved to the spectrometer. The cryostat, mounted on a movable platform, may be lowered gradually into the coil of the spectrometer probe. The cold surfaces inside the cryostat act as a cryopump and maintain the vacuum so that measurements can be taken for long periods of time (days). This method has the advantage that expensive cryogenic liquids are not required to reach the cryogenic temperatures.

Materials. Commercial argon, research grade acetylene, 1-propyne, 2-butyne, and allene were used without purification. Samples were diluted to 1:1 (v/v) with argon except for allene which was used neat.

Ketene was prepared[16] by passing vapor of commercial ketene dimer mixed with argon gas through a high-temperature vacuum oven at 650 °C and deposited directly onto the cryotip.

Commercial samples of 90 atom % ^{13}C-labeled carbon dioxide (CO_2), carbonyl sulfide (OCS), and carbon monoxide (CO) were diluted to 10% (v/v) with argon before use.

Carbon suboxide was obtained by the dehydration of malonic acid with P_2O_5 at 50 °C (1 mmHg) and collected in a vacuum trap at −80 °C. The carbon suboxide so obtained was used without further purification. The carbon suboxide vapor was codeposited with a 90–10% (v/v) argon–methane mixture.

Measurements. The Cross-Polarization Experiment. The use of the cross-polarization experiment in obtaining solid-state ^{13}C spectral data has been well documented in reviews.[17] Typically experiments are run with a 3-ms contact time for full polarization of all spins and a 3–5 s recycle time. Contact times as long as 10 ms are required to polarize carbons with very weak proton dipolar contacts.

The number of transients required to obtain usable spectra varies with sample concentration within the matrix. On a 50- to 100-mg sample, containing natural abundance ^{13}C, 25K transients are required to obtain a spectrum of usable quality. For samples of relatively high concentrations (e.g., isotopically enriched or >250 mg) useful spectra can be obtained in 500 transients. Typically 10K to 15K transients were satisfactory for most compounds. Spectra are referenced with an external sample of liquid Me_4Si at room temperature by substituting it for the cryogenic sample in the probe. The spectrum of Me_4Si is then obtained under identical spectrometer conditions. It is estimated that this type of external referencing could introduce errors as large as ±3 ppm in the chemical shift values, but the average of the tensor trace generally agreed with the respective liquid shifts much better than indicated by these error limits.

The Intermolecular Cross-Polarization Experiment. The intermolecular cross-polarization experiment (ICP) takes advantage of the presence of the easily polarizable protons in a molecule such as methane. It has been noted[18] that in the case of the hexamethylbenzene–tetracyanoethylene (HMB–TCE) complex, longer contact times increase the intensity of the TCE signal due to intermolecular cross polarization from HMB to TCE. Similar effects have also been observed in a matrix containing a mixture of solute, methane, and argon. A contact time of 10 ms was found to be optimal for most samples. Typically 20K to 25K transients are collected for this type of experiment as intermolecularly cross-polarized samples experience some reduction in signal sensitivity for otherwise comparable spin populations.

The use of methane in the matrix unfortunately creates a dynamic range problem. Since most nonprotonated molecules studied have exhibited large chemical shift anisotropies, the spectral intensity is spread over several hundred parts per million. The methane signal, on the other hand, is isotropic and very narrow in shape with a width at half-height of approximately 5 ppm and a base width of less than 25 ppm. Thus the methane signal tends to obscure signals in the region of 10 to −15 ppm, and it also poses a dynamic range problem as the spectra are scaled with spectral accumulation.

Attempts to improve the sample signal relative to the methane signal with dipolar dephasing[19] have proved unsuccessful. Apparently rapid motion of the methane molecule reduces the weak carbon–proton dipolar interaction, and thus the intensity of the methane signal is comparable to the nonprotonated signal intensities. Thus only modest CH_4 concentrations (~10%) in argon are feasible for intermolecular cross-polarization experiments even though CH_4 is otherwise a favorable cross polarizer because of its spectral simplicity and high proton spin density.

Spectral Analysis. ^{13}C chemical shielding values were obtained by comparing experimental spectra with numerically generated spectra obtained from the secular part of the chemical shift tensor.[17] A VAX 11/780 computer with PLOT79 graphics software was used for this task

(13) Pines, A.; Rhim, W. L.; Waugh, J. S. *J. Chem. Phys.* **1971**, *54*, 5438.
(14) Zilm, K. W.; Alderman, D. A.; Grant, D. M. *J. Magn. Reson.* **1978**, *30*, 563.
(15) Otteson, D.; Michl, J. *J. Org. Chem.* **1984**, *49*, 866.
(16) Fieser, L. F.; Fieser, M. "Reagents for Organic Synthesis"; John Wiley and Sons, Inc.: New York, 1967; Vol. 1.
(17) Mehring, M. In "High Resolution NMR Spectroscopy in Solids"; Diehl, P., Fluck, E., Kosfeld, R., Eds.; Springer-Verlag: Berlin-Heidleberg, 1976; NMR—Basic Principles and Progress, Vol. 11.
(18) Blann, W. G.; Fyfe, C. A.; Lyerla, J. R.; Yannoni, C. S. *J. Am. Chem. Soc.* **1981**, *103*, 4050.
(19) Opella, S. J.; Frey, M. H. *J. Am. Chem. Soc.* **1979**, *101*, 5854.

Table I. ^{13}C Chemical Shifts of Linear and Pseudolinear Molecules[a]

compd	$\sigma_\perp$ (I, II)[b]	$\sigma_\parallel$ (I, II)[b]	σ_{av} (I, II)[b]	σ_{iso}
CO[c]	305 (392, 361)	−48 (−58, −59)	187 (242, 221)	182.2
CO_2[d]	245 (262, 233)	−90 (−71, −75)	133 (151, 130)	132.2
COS[e]	275 (357, 299)	−90 (−97, −94)	153 (206, 168)	154.0
CS_2[d,f]	332 (488, 360)	−92 (−89, −99)	191 (296, 207)	192.8
$O{=}C{=}C{=}C{=}O$[g]	235 (253, *h*)	−90 (−73, *h*)	127 (144, *h*)	127.7
$O{=}C{=}C{=}C{=}O$[g]	24 (38, *h*)	−90 (−79, *h*)	−14 (−1, *h*)	−14.6
$HC{\equiv}CH$[d]	150 (157, 154)	−90 (−73, −77)	70 (80, 77)	71.9
$CH_3C{\equiv}CH$[i]	140 (149, 141)	−74 (−57, −59)	69 (80, 74)	68.4
$CH_3C{\equiv}CH$[i]	166 (164, 171)	−93 (−94, −97)	80 (78, 82)	79.8
$CH_3C{\equiv}CCH_3$[j]	152 (158, *h*)	−75 (−77, *h*)	76 (80, *h*)	74.8
	σ_{11} (I, II)[b]	σ_{22} (I, II)[b]	σ_{33} (I, II)[b]	σ_{ave} (I, II)[b]	σ_{iso}
$CH_2{=}CH_2$[k]	234 (285, 273)	120 (113, 113)	24 (0, 13)	126 (133, 133)	123.3
$CH_2{=}C{=}O$[l]	265 (305, 282)	239 (264, 249)	77 (58, 65)	194 (209, 199)	194
$CH_2{=}C{=}O$[l]	39 (92, 47)	4 (1, 3)	−27 (−22, −30)	3 (24, 7)	2.5
$CH_2{=}C{=}CH_2$[m]	158 (180, 173)	54 (55, 52)	23 (1, 12)	78 (79, 79)	74.8
$CH_2{=}C{=}CH_2$[m]	233 (236, 248)	233 (236, 248)	175 (172, 193)	214 (215, 230)	213.5

[a] All chemical shift values are referenced to external Me_4Si. Referencing and fitting procedures may introduce an error as large as ±3 ppm. [b] Theoretical chemical shift values are given in parentheses for two basis sets (I, II) relative to methane with absolute shielding values of 219 and 215 ppm for basis sets I and II, respectively. [c] Geometry used in the calculations obtained from: Herzberg, G. "Diatomic Molecules"; D. Van Nostrand Co., Inc.: Princeton, New Jersey, 1950; p 521. [d] Geometry obtained from: Herzberg, G. "Infrared and Raman Spectra"; D. Van Nostrand Co., Inc.: Princeton, New Jersey, 1945; p 398. [e] Geometry obtained from: Dakin, T. W.; Good, W. E.; Coles, D. K. *Phys. Rev.* **1947**, *71*, 640. [f] Shift values obtained from ref 14. [g] Geometry obtained from: Livingston, R. L.; Ranachandra Rao, C. N. *J. Am. Chem. Soc.* **1959**, *81*, 285. [h] The number of carbon and oxygen atoms in carbon suboxide and 2-butyne preclude theoretical results using basis set II for these two compounds. [i] Geometry obtained from: Costain, C. C. *J. Chem. Phys.* **1958**, *29*, 864. [j] Geometry obtained from: Tanimoto, M.; Kuchitsu, K.; Morino, Y. *Bull. Chem. Soc. Jpn.* **1969**, *42*, 2519. [k] Geometry obtained from: Allen, H. C.; Plyler, E. K. *J. Am. Chem. Soc.* **1958**, *80*, 2673. [l] Geometry obtained from: Moore, C. B.; Pimentel, G. C. *J. Chem. Phys.* **1963**, *38*, 2816. [m] Geometry obtained from: Maki, A. G.; Toth, R. H. *J. Mol. Spectrosc.* **1965**, *17*, 136.

in the manner described elsewhere.[20]

The numerically generated spectra were convoluted with a Lorentzian line width at half-height of about 2 ppm. While the generated and the experimental spectra were generally superimposable, at times minor deviations in intensities have been observed. In such instances, spectra which fit best at the shoulders and the prominent center peak are used to determine the tensorial shifts. The effect of magic angle orientations of the inter dipolar axes upon intensity was neglected in the calculations.

Theoretical Calculations of the Shielding Tensor. The chemical shift tensor was calculated for experimentally determined equilibrium geometries by a coupled Hartree–Fock method by using individual gauges for localized orbitals (IGLO).[21,22] Basis set I used a double-ζ (7,3) Huzinaga[23] set contracted to (4,1,1,1;2,1) on carbon and oxygen, (9,5) contracted to (4,1,1,1,1,1;2,1,1,1) on sulfur and (3) contracted (2,1) on hydrogen. Basis set II used the same primitive functions, but with a (5,1,1,1,1;3,1,1) contraction plus a d orbital with an exponent of 1.0 on carbon, oxygen, and sulfur and (3,1,1) contraction plus a p orbital with an exponent of 0.7 on hydrogen.

Results and Discussion

The tensorial chemical shifts for the molecules under study are given in Table I. In molecules with C_3 or higher rotational symmetry, the shielding tensors for atoms on the rotation axis exhibit axial symmetry and unequivocal spatial assignments follow directly from the twofold degeneracy in the principal shielding values.[17] Figure 1 presents the shielding powder pattern for 2-butyne which is representative of the axially symmetric pattern and in which the $\sigma_\perp$ and $\sigma_\parallel$ components are clearly determined from the two characteristic break points. The theoretical powder pattern and their convoluted form is also presented to indicate how the shift values are extracted from the powder pattern. In the overlapping patterns of the inequivalent carbons of propyne and 2-butyne (see Figure 1), the patterns of the methyl carbon are easily separated from the more diffuse patterns attributable to the alkyne carbons. In these axially symmetric molecules, the trace or $\sigma_{av} = (2\sigma_\perp + \sigma_\parallel)/3$ is in every case within the experimental error of the isotropic shielding value (σ_{iso}) determined for rapidly tumbling liquid samples. It is reassuring that the intermolecular interactions present in the solid matrix have not altered the shift values relative to the liquid phase within our error limits.

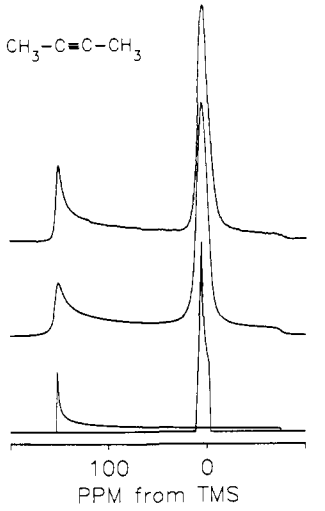

Figure 1. Carbon-13 spectra of 2-butyne: experimental, theoretical convoluted, and theoretical powder spectra are shown from top to bottom.

In ^{13}C-containing molecules with spherical or axial symmetry the shielding components may be unequivocally assigned from the intensity pattern. In molecules of lower symmetry this is no longer possible. There are six possible permutations for assigning the three principal values to three principal axes. In the most general case it is also necessary to specify the orientation of the principal axes in the molecular frame. The presence of a mirror plane passing through the ^{13}C nucleus establishes the normal as a principal axis, but the orientation of the two remaining axes in the mirror plane remains undetermined. Thus, the assignment of any one principal axis to a shielding value reduces the number of assignment permutations from six to two for the remaining two shielding parameters. Only one orientation angle instead of three remains to be determined. Thus any element of symmetry which permits one axis to be assigned greatly assists in the spatial characterization of chemical shielding tensors. Compared with the assignment of isotropic liquid shifts (one value for each uniquely different nuclear spin), the spatial designation of shielding tensor values is considerably more challenging. Until theory or precedent provides a reliable basis for making such spatial assignments of new tensorial shifts, considerable care should be exercised in cataloging tensorial shifts.

(20) Zilm, K. W. Ph.D. Dissertation, University of Utah, 1981.
(21) Kutzelnigg, W. *Isr. J. Chem.* **1980**, *19*, 193.
(22) Schindler, M. S.; Kutzelnigg, W. *J. Chem. Phys.* **1982**, *76*, 1919.
(23) Huzinaga, S. "Approximate Atomic Wave Functions"; University of Alberta: Edmonton, Alberta, 1971.

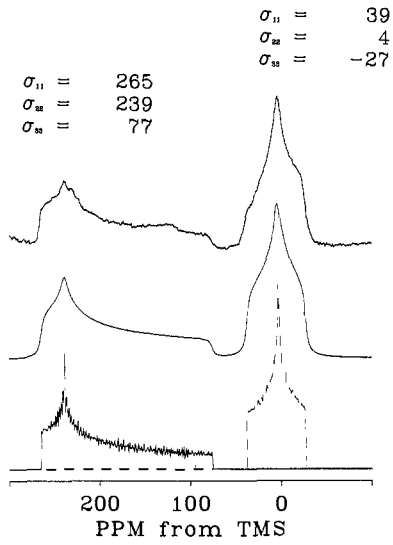

Figure 2. Carbon-13 spectra of ketene: experimental, theoretical convoluted, and theoretical powder pattern spectra are shown from top to bottom. The fluctuations in the theoretical powder spectrum are due to the finite number of points used in its calculation. With the broadering such fluctuations are eliminated.

One of the most interesting results observed in this work is the preponderance of the −90-ppm value for $\sigma_\parallel$ in molecules containing a C_∞ symmetry axis. Only for CO was a value of −48 ppm observed for $\sigma_\parallel$. A sound theoretical basis[24,25] depending only upon symmetry arguments exists for the similarity of $\sigma_\parallel$ values in linear molecules which have a $^1\Sigma$ ground state. In such molecules, the paramagnetic shielding contribution vanishes when the magnetic field is aligned along the principal molecular axis leaving only the diamagnetic component to vary. It should be stressed that the −90-ppm value does not represent zero shielding, however, as the diamagnetic component is not negligible (several hundred parts per million). It is significant to note from the molecules studied that the diamagnetic component of $\sigma_\parallel$ must be relatively constant and for many linear molecules is within the experimental error of ±3 ppm. This is somewhat surprising considering the variety of directly bonded atoms (H, C, O, S) present in this set of compounds. The results are supported by theoretical work[26] which indicates that the atomic diamagnetic term is reasonably constant among differing molecules. This conclusion depends upon a selection of gauge in the calculation which would not reapportion the diamagnetic and paramagnetic terms in some artificial way. Except for CO, the data on $\sigma_\parallel$ of these C_∞ molecules indicate that only minor variations may be ascribed to the diamagnetic term where the paramagnetic term is zero. For these reasons, the −90-ppm position may be considered to be a zero fiducial mark for paramagnetic shielding components. Admittedly, the diamagnetic term can influence the shifts in ionic species and molecules with high charge polarization, but these variations will in general be smaller than typical paramagnetic contributions to shielding.

Shielding terms arising from electrons on adjacent atoms can also contribute to minor variations in shielding, but these off-center terms will affect all magnetic nuclei to the same extent, provided that the various shielded nuclei are positioned at the same place in a molecule. As these contributions also would affect shielding in protons, the proton shielding range of 10 ppm places an upper limit on the off-center terms. The carbon tensorial shifts primarily reflect the variations in the dominant paramagnetic shielding term which is sensitive only to electronic states exhibiting angular momentum components (e.g., p and d electrons) centered on the shielded nucleus. As Table I contains shielding data covering almost the entire known ^{13}C chemical shift range, the linear molecules are sufficiently representative to provide a set of compounds on which a reasonable number of general conclusions can be based concerning chemical shielding. This broad range is rather remarkable when the similarity of chemical types of carbons is considered.

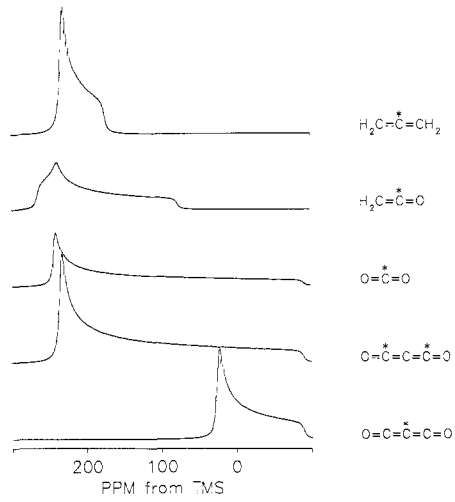

Figure 3. Variations of $\sigma_\parallel$ and $\sigma_\perp$ for allene, ketene, carbon dioxide, and carbon suboxide. These spectral simulations illustrate the dramatic range in shifts and the effect that changes in molecular symmetry have upon of the chemical shift tensor.

The presence of hydrogens off the symmetry axis in the pseudolinear molecules is sufficient to cause significant deviations from the −90-ppm fiducial value and clearly documents the importance of symmetry in chemical shielding. Figure 2 illustrates typical asymmetric bands in the spectrum obtained for ketene. Ketene is isoelectronic with CO_2 and allene, and data for all three are given in Table I. Spectral data for these three compounds illustrate both the role that symmetry plays in the overall range of the chemical shift tensor and the dramatic changes in shift values associated with the presence of protons off the principal axis. Precedent exists for such variations in the chemical shift tensor element associated with the C–C bond direction in ethylene (129 ppm) and acetylene (−90 ppm) where one observes a difference of 219 ppm (see Table I) due largely to symmetry quenching of the paramagnetic term in acetylene.[27] The effect of breaking the symmetry is even more surprising for the central atom of the isoelectronic species O=C=O, CH_2=C=O, and CH_2=C=CH_2 where the off-center protons are not even bonded directly to the atom of interest. Note the significant variations in the shielding component associated with the long axis of these molecules with the value of $\sigma_\parallel$ changing from -90 ppm in carbon dioxide to 77 ppm in ketene and finally to 175 ppm for the central carbon of allene—a remarkable variation of 265 ppm. By comparison, the corresponding $\sigma_\perp$ varies by a comparatively small amount: CO_2, 243 ppm; ketene, 265/239 ppm; allene, 233 ppm. Figure 3 illustrates the variation in ^{13}C chemical shielding tensors for the central carbon of this isoelectronic series of molecules and compares these data with those obtained for the two carbons in carbon suboxide, C_3O_2. The shielding tensor values for C_1 and C_3 in C_3O_2 are remarkably similar to those of CO_2, but the pattern for C_2 differs greatly from that of the other molecules in Figure 3 due to $\sigma_\perp$ having such a high field value. This notable variation in the $\sigma_\perp$ component (24 ppm) found for the central carbon of carbon suboxide compares with 235 ppm for the terminal carbon in C_3O_2, 243 ppm for carbon dioxide, and 233 ppm in allene, C_3H_4. As the central carbon in both C_3O_2 and C_3H_4 exhibits a similar cummulated carbon skeleton, the result is of considerable interest. Substitution of oxygen in CO_2 with sulfur causes $\sigma_\perp$ to shift to lower field in a monotonic and fairly linear manner.

In methylacetylene, the terminal alkyne carbon has a downfield shift of 15 ppm in $\sigma_\parallel$ while $\sigma_\perp$ is essentially unchanged. Presumably this is due to methyl protons which are three bonds

(24) Ramsey, N. F. *Phys. Rev.* **1950**, *78*, 699.
(25) Ramsey, N. F. *Phys. Rev.* **1951**, *83*, 540.
(26) Grutzner, J. B.; Nowicki, N. R., private communication.
(27) Pople, J. A. *Proc. R. Soc. London, Ser. A*, **1957**, *239*, 541.

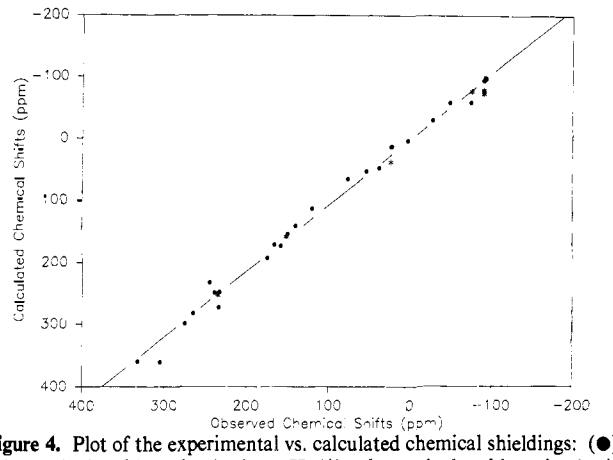

Figure 4. Plot of the experimental vs. calculated chemical shieldings: (●) values calculated by using basis set II, (*) values calculated by using basis set I. The experimental values are referenced to Me_4Si and the calculated ones to methane as is explained in Table I.

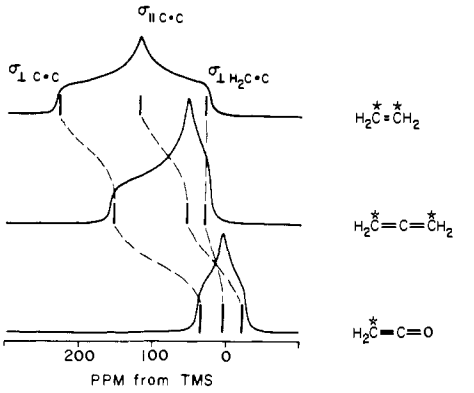

Figure 5. Carbon-13 chemical shift tensor for the methylene carbon in ketene, allene, and ethylene. Dashed lines indicate the tensor components associated with related spatial components. Note that the relative invariance of the component perpendicular to the H–C–H plane results in a crossover of $\sigma_{\parallel C=C}$ and $\sigma_{\perp H_2C=C}$.

removed from the carbon of interest and which are even more remote than those in ketene and allene. Thus, the effect of molecular symmetry on even remote shielding electrons can produce notable variations in the shifts.

In order to assist in the spatial assignment of the shielding tensor, when symmetry arguments are unavailable, and to gain insight into the origin of such shifts, ab initio calculations (see Table I) were performed by the IGLO version of the coupled Hartree–Fock method.[21,22] For the cases in which the assignments are determined unequivocally by symmetry considerations, the method correlates the results very well (see Table I). Thus, there is reason to believe that the theoretical calculations substantiate the assignments given in Table I for the other molecules. In Figure 4 the observed shifts are plotted vs. the theoretical ones calculated by using the large basis set (II), except in carbon suboxide and 2-butyne where those obtained with the small basis set (I) are shown. The pairing of theoretical with experimental shifts was, in every instance, selected so that the ordering of tensorial values would be the same for a given nucleus. With this assumption an excellent correlation was observed with a scatter not exceeding a 20-ppm range. An excellent correlation is observed between the experimental and calculated values, when the larger basis set II is used. The least-squares fit, shown as a solid line in Figure 4, gives a slope of 1.0648, an intercept of 0.8929, and a correlation coefficient of 0.9959. Respective values of 1.1309, 5.2721, and 0.9831 were obtained for basis set I. It should be noted that the major improvement of the results obtained by using the large basis set (II) results almost entirely from the molecules containing sulfur where the small basis set introduces major discrepancies.

The calculations are very useful for making assignments. For example, one must depend upon them to provide the assignments for the terminal carbon in allene and for both carbons in ketene. The middle carbon in allene may be assigned on the basis of its axially symmetric tensor. The calculated shielding values fortunately agree sufficiently well with only one permutation of the experimentally observed values to feel fairly confident of the assignments. When two or more of the tensorial components are relative near one another (e.g., both carbons in ketene and the CH_2 of allene; see Table I) these assignments should only be taken as tentative for the present. Figure 5 compares such assignments for ketene and allene with the previous results on ethylene, where the orientation of σ_{22} was determined experimentally.[7] For a given structural feature the shifts vary in a regular and monotonic manner. The spatial orientation of a given shift value is specified by the labels in Figure 5. Note that the two mutually perpendicular mirror planes in ethylene, allene, and ketene specify all of the angles of the principal axes relative to the molecular framework. Thus, only the correct permutational order of the shifts with the different axes is required from the theoretical method. The experimental shifts can be assigned to the molecular axes even though the theoretical magnitude could be in error providing the ordering of the shifts is reliable. The spatial ordering of the chemical shift tensor for the CH_2 carbon of ketene differs from that in either allene or ethylene as may be seen in Figure 5. In the chemical shift tensors of ethylene and allene σ_{11} is oriented perpendicular to the long axis of the molecule but contained in the plane of the CH_2 moiety ($\sigma_{\perp C=C}$), σ_{22} is parallel with the long axis of the molecule ($\sigma_{\parallel C=C}$), and σ_{33} is perpendicular to the CH_2 plane ($\sigma_{\perp H_2C=C}$). The theoretical orientation for ketene has σ_{22} perpendicular to the CH_2 plane ($\sigma_{\perp H_2C=C}$) and the high-field σ_{33} parallel to the long axis of the molecule ($\sigma_{\parallel C=C}$). Only for the lowest field σ_{11} component of the ketene shift tensor is the spatial orientation of its principal axis the same as in allene and ethylene. This crossover in the shielding values for the series ethylene, allene, and ketene is shown in Figure 5.

The trigonal symmetry of the methyl group in propyne and 2-butyne preserves the axial shielding tensors of the acetylene linkage and all shielding values can be assigned to the molecular axes unequivocally. Having assigned the chemical shielding tensor in this series of acetylenes, one can observe some interesting effects of methyl substitution. Since tensorial components depend primarily upon electron motion in the plane perpendicular to the component's direction,[28] it can be determined that $\sigma_{\parallel}$ depends on the π-electron behavior and $\sigma_{\perp}$ monitors both σ and π electrons at the carbon of interest. Examination of charge density calculations on the three acetylenes of interest reveals that trends in direction and magnitude of both σ_{iso} and $\sigma_{\perp}$ are reflected in changes in both σ and π charge density. Changes in $\sigma_{\parallel}$ correspond to variations in π-electron density but to a lesser extent.

In conclusion, this series of linear and pseudolinear molecules provides a reasonably comprehensive study of shielding tensors in a series of well-defined systems. The uniqueness of the −90-ppm value for many $\sigma_{\parallel}$ can be understood as the paramagnetic term vanishes due to symmetry, and it implies a constancy in the diamagnetic shielding terms even though substituent atoms vary from H, C, O, to S. Calculations have been found to agree quite closely with experimental results when no ambiguity exists in the assignments, giving confidence in those assignments which for the time being must totally rely on theoretical calculations. Chemical shift tensors obtained for a variety of molecules such as allene and ketene were found to provide unusual examples of the effect of breaking the C_∞ symmetry of the molecule. These findings dramatize the importance of symmetry in structural analysis based on tensorial shifts and portend high promise for these kind of data in structural characterization of molecules.

Acknowledgment. This work was supported by the National Science Foundation (CHE 83-10109).

Registry No. CO, 630-08-0; CO_2, 124-38-9; OCS, 463-58-1; C_3O_2, 504-64-3; C_2H_2, 74-86-2; $CH_3C{\equiv}CH$, 74-99-7; $CH_3C{=}CCH_3$, 503-17-3; $CH_2{=}C{=}CH_2$, 463-49-0; $CH_2{=}C{=}O$, 463-51-4.

(28) Strub, H.; Beeler, A. J.; Grant, D. M.; Michl, J.; Cutts, P. W.; Zilm, K. W. *J. Am. Chem. Soc.* **1983**, *105*, 3333.